Magnetic Resonance in Medicine 41:727–733 (1999)

Diffuse Axonal Pathology Detected With Magnetization Transfer Imaging Following Brain Injury in the Pig

Joseph C. McGowan,[1]* Timothy M. McCormack,[1] Robert I. Grossman,[1] Renato Mendonça,[1] Xiao-Han Chen,[3] Jesse A. Berlin,[4] David F. Meaney,[2] Bai-Nan Xu, Kim M. Cecil,[1] Tracy K. McIntosh,[3] and Douglas H. Smith[3]

This study was designed to evaluate with magnetization transfer imaging (MTI) and conventional magnetic resonance (MR) imaging the manifestation of diffuse axonal injury (DAI) in an animal model of injury via nonimpact coronal plane rotational acceleration. A second objective was to investigate the diagnostic use of quantitative MTR imaging based on statistical parameters in a single subject, as opposed to grouped analysis. Seven mini-swine were subjected to brain trauma known to produce isolated DAI and to MR imaging at two time points. Following sacrifice, the brains were harvested for histopathologic examination. Magnetization transfer ratio (MTR) maps were generated for double-blinded comparison of regions with abnormal MTR values and regions with documented DAI. Positive and negative predictive values for MTR detection of DAI were 67 and 56%, respectively, and in acute studies alone, 89 and 61%. Gains in sensitivity over conventional imaging for detection of DAI were demonstrated. Magn Reson Med 41:727–733, 1999. © **1999 Wiley-Liss, Inc.**

Key words: brain, abnormalities; brain, MR; brain, white matter; magnetic resonance; magnetization transfer contrast

Traumatic brain injury (TBI) affects in excess of 2 million victims par year in the United States and is the leading cause of death in children and young adults (1,2). Common sequelae include both focal and diffuse pathologies, the latter including lesions in white matter described as diffuse axonal injury (DAI). Occurring secondary to inertial forces that rotate or otherwise deform the brain, DAI is manifest as a characteristic pattern of injury related to the physical constraints of cerebral anatomy; it results from the stresses and strains that accompany rapid deformation. Motor vehicle accidents are commonly the cause of such injury. Diffuse axonal injury may be distinguished from focal brain injury, which is commonly associated with impact to the head and contact, rather than inertial loading forces, Focal brain injury is typically characterized as cerebral contusion and hematoma (3). Moderate to severe DAI is associated with approximately a third of deaths in severely head-injured patients and is thought to be responsible for poor neurologic outcome in many survivors of head injury (3,4).

Evaluation of patients with TBI is complicated by the inability of current imaging methodologies to detect the full extent of DAI, in particular at a level where damage is not life-threatening but is serious enough to result in loss of consciousness as well as mild to severe cognitive and neurologic motor deficits. As new techniques for brain imaging are introduced, offering the promise of a more sensitive examination, it becomes advantageous to investigate imaging results that can be compared with a reference standard such as histopathologic analysis. Additionally, it is desirable to investigate techniques that may be sensitive to pathology not demonstrated by histopathologic analysis, perhaps due to limitations of the particular staining techniques employed.

Magnetization transfer imaging (MTI) is designed to generate contrast based on the exchange of proton magnetization between water molecules and macromolecules in tissue (5). It represents a normalized, quantitative, imaging technique in that a magnetization transfer ratio (MTR) may be associated with every location in an imaged volume of tissue (6). Quantitative analysis of MTI has demonstrated the potential for increased sensitivity in the detection of structurally compromised white matter in animal models of Wallerian degeneration (7), and experimental allergic encephalomyelitis (6), and in human multiple sclerosis (6,8,9), metastatic disease (10), and periventricular multifocal leukomalacia (11). Previous studies, including most of those cited above, have relied on analysis of grouped data to detect differences between injured and normal populations with MTR. In contrast, our previous work (11) made use of contour plotting of MTR values, to delineate areas of abnormal MTR based on statistical variation from normal. This study represents the first known attempt to apply a similar technique to the investigation of potential diagnostic efficacy of the MTR and related parameters by using an animal model with available histopathologic analysis and a double-blind design.

A challenge to the investigation of TBI is the difficulty of inducing isolated DAI in an animal model, that is, DAI without concomitant contusion. Previously, it has been demonstrated that rotational acceleration of the brain immediately following the injury event produces mechanical loading that results in DAI (12). The inertial loading of the brain results in the development of compressive and tensile strain forces as well as shearing forces, all leading to deformation. Thus, a suitable animal model for DAI must have a brain size sufficient to be significantly accelerated within the limitations of mechanical equipment, and must

[1]Department of Radiology, University of Pennsylvania, Philadelphia, Pennsylvania.

[2]Department of Bioengineering, University of Pennsylvania, Philadelphia, Pennsylvania.

[3]Department of Neurosurgery, University of Pennsylvania, Philadelphia, Pennsylvania.

[4]Center for Clinical Epidemiology and Biostatistics, University of Pennsylvania, Philadelphia, Pennsylvania.

Grant sponsor: NIH; Grant numbers: NS08803 and NS34353.

*Correspondence to: Joseph C. McGowan, Department of Radiology, University of Pennsylvania, 3400 Spruce St., Philadelphia, PA 19104.
E-mail:jmcgowan@seas.upenn.edu

Received 16 June 1998; revised 20 August 1998; accepted 28 September 1998.

© 1999 Wiley-Liss, Inc.

also possess a brain geometry that may be related to human anatomy. For these reasons, we chose a rotational acceleration injury that has been demonstrated to produce mild to moderate isolated DAI in mini-swine (12,13). We induced DAI in this model and evaluated the progress of brain injury over a 1-week period with conventional MR imaging and MTI, followed by sacrifice and histopathologic examination. Our hypothesis was that MTR results would reflect structural injury as demonstrated by histopathologic analysis.

MATERIALS AND METHODS

Eight miniature young adult (4 months of age) swine (Hanford strain), both male and female, weighing 18–22 kg, were used in this study. Seven animals received injury by non-impact, coronal plane, rotational acceleration, and one served as an uninjured control. All animal procedures were approved by the University of Pennsylvania Animal Care and Use Committee, and we carefully adhered to the animal welfare guidelines set forth in the *Guide for the Care and Use of Laboratory Animals,* US Department of Health and Human Services Publication 85-23. Animals received MR imaging approximately 3 days before injury, immediately following injury (the acute study), and at 7 days following injury (the D7 study). The animals were fasted for 12 h prior to injury or imaging. Anesthesia was induced with an initial injection of midazolam (400–600 mg/kg) followed by 2–4% isoflourane via a snout mask until a plane of surgical anesthesia was reached. The animals were intubated endotracheally and maintained on 1.5–2% isoflourane for the entire duration of the injury or imaging protocol. Previous experience with this animal model and extensive monitoring indicated that no substantial physical changes should be expected in the model either prior to or following injury (13). Thus, monitoring in the study group consisted of pulse oximetry from the skin of the tail, a rectal thermometer for core body temperature, and end-tidal CO_2 measurement from the endotracheal tube. One of the seven injured animals received the acute and D7 scans but was not imaged prior to injury. An eighth animal was uninjured and was included in the analysis of average pre-injury deep white matter MTR. At 7 days following brain injury, the animals received the final MR examination and were then given an overdose of pentobarbitol (150 mg/kg, IV). Histopathologic analysis was performed, and the results were compared with the results of quantitative MTI analysis as well as with a conventional reading of the MR scans. The investigators performing the conventional MR, histopathology, and MTR analyses were all blinded to the others' results. Details of the procedural steps are given below.

Injury Induction

The rotational injury apparatus, known as the HYGE pneumatic impactor, was previously described in detail (14). Producing 20,000 kg of thrust, it was modified from that used to induce DAI in non-human primates characterized by brain weights approximately equal to those in the current animal model (4). The anesthetized animals were secured to the apparatus via a padded snout clamp, which was attached directly to the HYGE linkage. The apparatus was configured to produce a pure impulsive head rotation in the coronal plane, with the center of rotation close to the center of mass. Inhalation anesthesia was withdrawn approximately 10 sec before activation of the injury device. The impulse of the device caused the head to rotate through 105° in 20–30 msec, with a predominant deceleration component during the rotation. Following injury, the animals were released from the apparatus, and vital signs were monitored. Upon stabilization (less than 15 min following injury), the animals were extubated and were continuously monitored for respiration and pulse until they were awake and ambulatory, which was always within 1 h of injury. Buprenorphine (0.1 mg/kg, i.m., q 12 h. p.r.n.) was given for post-injury analgesia.

Magnetic Resonance Imaging

The imaging protocol was carried out in a clinical 4 T MR scanner (GE Medical Systems, Milwaukee, WI) using a product quadrature transmit/receive head radiofrequency coil. The pig was placed in the scanner on top of a vacuum-fixation blanket, which was used to standardize its position on repeat studies. Ventilation with 1.5–2% isoflourane and pulse oximetry were maintained throughout the study. Conventional MR imaging of the pig brain consisted of a sagittal T1-weighted localizer, and T2-weighted fast spin echo (FSE) with TR 6000 msec, TE_{eff} 68, echo train length 4, 3 mm slice thickness with 2.5 mm between slices, matrix 256 × 128, and 1 excitation per phase-encode step. Imaging time was 6:48 for this scan. MTI was performed with a modified three-dimensional gradient-echo sequence, which was provided as part of the GE vascular imaging package. Sequence parameters included TR 106 msec, TE 5 msec, flip angle 12°, 3 mm section thickness, matrix 256 × 128, and a square field of view FOV 16 cm on a side. A control scan was acquired without MT saturation, using the above scan parameters, which were chosen to develop primarily proton-density weighting. Each of the two scans for MR analysis required 7:17 mins. MT saturation was given as off-resonance pulsed excitation consisting of a single sinc-shaped pulse per TR at equivalent flip angle 700°, offset 1200 Hz upfield of resonance. Images with and without MT saturation were subjectively evaluated on the scanner and overlaid to verify that the animal did not move between or during acquisitions; unsatisfactory scans were reacquired when necessary.

Spin-echo images were evaluated for the presence of DAI by a board-certified neuroradiologist (R.I.G.). Image analysis of the MT studies was carried out off-line using custom software written in interactive data language (IDL, Research Systems, Boulder, CO). Six central slices with corresponding MT control images were selected on each animal, to include all the deep white matter tracts. Pixel locations for analysis were identified as those in the control image where intensity exceeded 5% of the maximum intensity, to screen out background and noise and to eliminate subsequent problems of division by zero. The set

of pixels remaining in each slice of interest was used to calculate MTR as follows:

$$MTR = \left[1 - \frac{M_s}{M_o}\right] \cdot 100\% \quad [1]$$

where M_s is the pixel intensity on the MT image and M_0 the corresponding intensity on the control image. MTR represents the suppression of image intensity due to the off-resonance saturation pulse and is normalized by proton density. The MTR maps that resulted from this analysis were analyzed in two ways. First, regions of interest were chosen in areas of deep white matter on the pre-injury studies. These areas are known to be susceptible to DAI through prior experience with this model. Second, contour maps were superimposed on the MT images to outline boundaries of MTR 2 or more standard deviations below pre-injury MT values. The contour maps were employed due to their ability to demonstrate well-defined regions of reduced MT, which are inapparent on visual examination, as well as to show the boundaries of regions that can be seen to be injured on the raw images or MTR maps. As noted, MT scans were available for two time points, representing acute injury and injury at the 7-day point.

Histopathologic Analysis

Following euthanasia, the descending aorta was clamped and transcardially perfused with 4 L of saline followed by 10 L of 4% paraformaldehyde. The brains were removed, postfixed in 4% paraformaldehyde for 2 h, stored in phosphate buffer solution, and cryoprotected with sucrose. The brains were blocked into 0.5 cm coronal sections for gross examination and photography. To the extent possible, the cutting was performed such that representative blocks, although they were several orders of magnitude thinner, corresponded to the anatomic images obtained from the pigs at the final MR examination. A series of 40 μm frozen sections was cut from the front face of each block and mounted on slides for microscopy. Adjacent sections evaluated with immunohistochemical techniques using the N52 antibody, targeting the 200 kD neurofilament subunit (Sigma 1:400) and the SMI-31 antibody, targeting selected epitopes located primarily on the 170–200 kD neurofilament subunits. The sections were incubated with primary antibody overnight at 4°C and then incubated at room temperature for 1 h, each with the appropriate secondary antibodies and ABC solution (1:1000). Peroxidase activity was revealed with 0.025% 3,3′-diaminobenzidine, 300 mg imidazole, and 0.25% H_2O_2 for 10 min. The sections were examined under light microscopy to determine the extent and distribution throughout each section. An ordinal rating scale was employed, based on the numbers of damaged axons/anatomic region/section. Hence, on the basis of histopathology only, injury was classified as mild (1–5 damaged axons), moderate (6–15 damaged axons), and severe (>15 damaged axons) (13).

Comparison of MTR With Histopathological Results

To provide a comparison between the quantitative MTR results and the semi-quantitative histopathologic results, a binary determination of injured/not injured was chosen. Injury on MTR was defined as a region of deep white matter with average MTR at least 2 standard deviations below pre-injury average values. Only regions that were completely surrounded by tissue having MTR in the normal range were included, to minimize the effects of partial volume averaging. On MTR maps that demonstrated injury by MTR, individual regions were identified, and their locations were transferred to a hard-copy image depicting the anatomy of the section. In addition, at least an equivalent number of sham locations in deep white matter were drawn on the hard-copy image. In all, 42 injured regions were identified in images from the seven injured animals, an average of seven per animal, and no such regions were identified in images from the control animal. A total of 80 sham locations was designated. The hard-copy annotated images were provided to the investigators who had previously analyzed the histopathologic sections but were blind to the MR results. They were asked to determine which of the identified locations corresponded to regions in which they had detected injury. One of four possible outcomes was assigned to each location, corresponding to elements in a standard 2 × 2 decision matrix.

Statistical Analysis

Values of MTR in normal deep white matter on the pre-injury studies were compared among animals by analysis of variance. To summarize the relationship between MTR on the post-injury studies and histologic findings, we constructed separate contingency tables for the overall results, the acute findings, and the D7 findings. Although typically used to summarize patient-level data, diagnostic test characteristics were used to describe the region-specific results. The positive predictive value for each table was defined as the probability of a positive histologic finding given that the MTR finding was positive. Similarly, the negative predictive value was defined as the probability that the histology was negative given that the MTR was negative. Each of these probabilities was estimated from each sample, along with a 95% exact binomial confidence interval. The statistical significance of the association between the MTR and histologic findings was tested using the ordinary Pearson chi square for the overall findings and the D7 findings. All *P* values reported were two-sided. For the acute findings, because one of the expected cell counts for the 2 × 2 table was less than 5, two-sided Fisher's exact probability was calculated. Analyses were performed using the STATA (ver. 5.0, Stata, College Station, TX) statistical software package.

Because the distribution of positive and negative MTR findings sent for histologic assessment was not random with respect to the distribution of positive and negative regions in the entire brain, the sensitivity and specificity of MTR could not be calculated from the observed data without bias. The particular form of bias is sometimes termed verification bias; it arises when the result of the test being evaluated (the index test) is used to determine which individuals have that test result verified. This may be understood by considering that, in clinical settings, the likelihood of a patient being sent for verification by a gold standard test is much higher for patients with positive index tests than for those with negative index tests. In this situation, the bias-corrected sensitivity will be lower than the uncorrected value calculated by conventional means, whereas the bias-corrected specificity will be higher than

the uncorrected value (15). To avoid verification bias, the results of the present study are given as positive (PPVs) and negative predictive values (NPVs), that is, as the likelihood of a certain pathology finding given a certain MTR result.

RESULTS

Prolonged coma was not produced in this model, consistent with earlier swine results. A transient (<15 min) loss of consciousness followed injury and may have been exacerbated by anesthesia. The animals were ambulatory within a few hours of injury, but they appeared somewhat disoriented for up to 6 h following injury. By 24 h after injury, the animals were grossly asymptomatic. Diffuse axonal pathology was present in all animals subjected to the rotational acceleration protocol, as evidenced by histopathologic evaluation and was not present in the control animal. Additionally, each injured animal was found to have at least one concordant positive pair of findings, an MTR abnormal area matching an area of confirmed pathology on double-blinded comparison. The axonal pathology observed included axonal bulbs (terminal clubbing) and axonal swelling, similar to that manifested in humans and non-human primates. Examples illustrating the type and magnitude of observed pathology are shown in Fig. 1. The most extensive axonal injury was present in deep white matter tracts at the root of the gyri, and at the gray-white matter junctions in the frontal, parietal, temporal, and occipital lobes. Axonal pathology was also present at the margins of lateral ventricles, external capsules, cerebral peduncles, and basal ganglia.

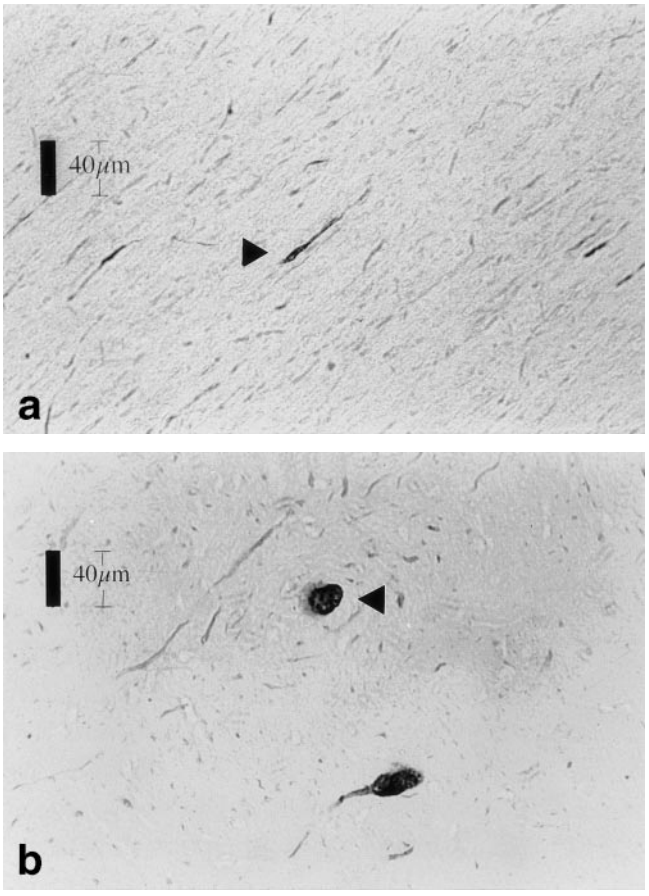

FIG. 1. Representative axonal pathology (arrowheads) including axonal swelling (**a**) and terminal clubs (**b**) found in deep white matter regions analyzed for MTR. The figures show one field at ×20 magnification, with length scale as shown.

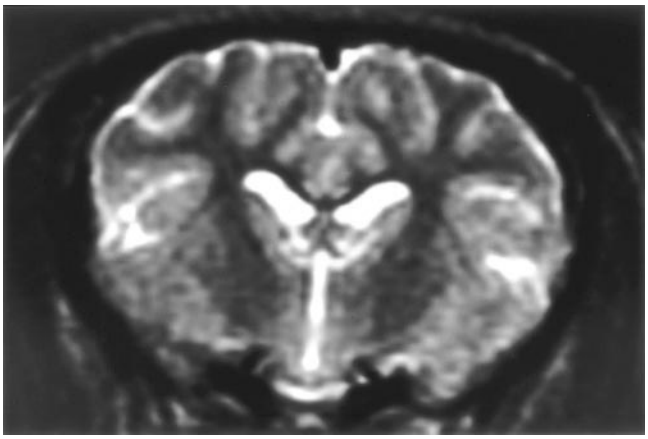

FIG. 2. Conventional T2-weighted MR image acquired with a fast spin-echo pulse sequence, TE_{eff} 64 msec, TR 6000 msec, echo train length 4, slice thickness 3 mm, and total acquisition time 6:48 for 30 slices. This image was acquired within 2 h of injury.

All the T_2-weighted scans were negative for DAI as read in the conventional manner. Figure 2 is an example of a FSE image obtained in the acute study of one animal. The average MTR value in deep white matter prior to injury was 39.4 ± 2.1 (mean ± SD), and there were no differences between animals in individual values for normal white matter MTR by analysis of variance. In all, 42 regions were identified as MTR-abnormal, and in each of these regions the measured MTR was between 2 and 4 SD below normal. Adjacent slices were examined when abnormal areas were identified to exclude regions potentially contaminated by partial volume effects of cerebrospinal fluid. Figure 3 depicts a contour plot from a D7 study; circumscribed regions of abnormal MTR are seen outlined by contours 2 SD below normal. In addition to the identified MTR-abnormal regions, 80 sham regions were selected, and hard-copy maps showing all 122 regions were provided to the histopathology team. Results of the comparison and relevant statistical measures are shown for three separate contingency tables (combined in Table 1). The PPV was 67% for the entire sample. The corresponding NPV was 56%. Considering only the MTR-identified regions and sham locations on the acute studies, the PPV was 89%, and the NPV was 61%. For the D7 studies considered independently, PPV was 61%, and NPV 52%. The association in the D7 subsample was not significant. All the abnormal MT results fell within the range of 2–4 SD below normal, and 61/63 of the regions judged injured by histopathology were graded as mild, with the remaining two graded moderate.

The uncorrected sensitivity and specificity for MTR in the detection of pathology-proven DAI were 44% and 76%, respectively. Considering only acute studies, the uncorrected sensitivity and specificity were 36% and 96%, respectively. As noted, the effect of verification bias due to the study design tends to lower the observed specificity and to raise the observed sensitivity. Thus, the observed values of sensitivity and specificity represent upper and

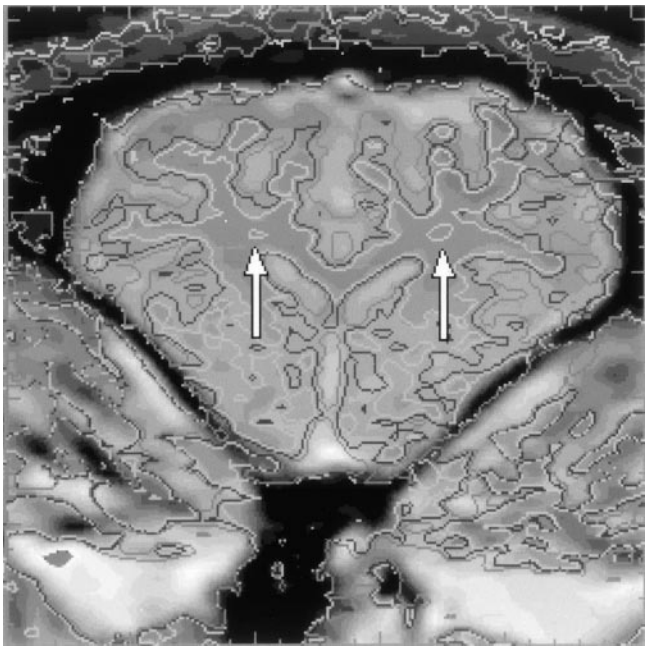

FIG. 3. Magnetization transfer ratio contour plot. Contours of MTR 2, 4, and 6 SD below normal are superimposed on the MTR map. Two regions of abnormally low MT are seen in deep white matter (arrows). These regions were found to correspond to confirmed DAI by histopathology.

lower bounds, respectively. This follows from the observation that a region with a positive (i.e., abnormal) MTR result was 100% likely to be subjected to comparison with the histopathologic results, whereas, considering all areas with negative MTR results, any particular area was less likely to be chosen for verification (15).

DISCUSSION

Human DAI occurs primarily in three major anatomic areas: lobar white matter, corpus callosum, and dorsolateral aspects of the rostral brainstem (16–18). The hallmark pathologies of DAI include axonal swelling and axonal bulbs, both of which were observed to be present in this animal model. It is not known whether these two manifestations of DAI represent a progression of injury or distinct injury processes progressing in parallel (19–21), but in our experience they are not found in isolation. We detected axonal swelling extending up to several hundred microns, often having multiple varicosities along the length of the axons. Axonal bulbs were seen as spherical structures tapering down to an almost normally sized axon proximally and ligated distally. The extent of axonal pathology induced with our injury model is relevant to the investigation of human head injury, and the amount and diffuse distribution of axonal injury found in this study was judged to be similar to mild-moderate DAI in humans.

Table 1
Contingency Table for Magnetization Transfer Detection of Injury Compared With Histopathology

	Histopathology					
	Entire sample		Acute studies only		D7 studies only	
	+	−	+	−	+	−
MT						
+	28	14	8	1	20	13
−	35	45	14	22	21	23
P	0.016		0.01			0.26
X^2	5.79		7.20			1.26
PPV	67%		89%			61%
95% CI[a]	50	80	52	100	42	77
NPV	56%		61%			52%
95% CI[a]	45	67	43	77	37	68

[a]Exact 95% binomial confidence interval.

Our results suggest that MTR analysis as we applied it is a relatively specific test for pathology-proven mild DAI. This is encouraging in light of the fact that no hemorrhagic lesions or other focal abnormalities were detected on review of the T_2-weighted and proton-density weighted FSE images. It is possible that small hemorrhagic lesions were present in the acute time period and resolved by the time of sacrifice. These might have been detectable with an optimized gradient-echo sequence designed to do so, but such lesions were not the focus of this study design, and in fact the better PPV and NPV associated with the acute studies alone suggest that the presence of such lesions was not important to the reported outcome. The ability of MTR to identify axonal changes in this study is even more remarkable considering that the regions selected for MTR analysis contained relatively minor axonal damage, as a result of our restriction on the selection of MTR regions to those that were surrounded by normal tissue. This restriction was imposed to avoid partial volume errors, even though injury was expected, and later confirmed, to be more extensive in areas along anatomic boundaries. The changes in MTR that we observed were less overt in magnitude when compared with those previously seen in other disorders of the brain, such as multiple sclerosis (6).

A significant anatomic difference between this animal model and humans is the much smaller falx present in the mini-swine. We observed no macroscopic tearing of midline structures as a result of the rotational acceleration injury, in contrast to that which would be expected in humans. During coronal plane rotation in humans, the falx may serve to ''tether'' the brain at its midline and thus to contribute to damage to midline structures such as the corpus callosum (13,22).

Comparing scans at two different time points, we noted more extensive areas of MTR abnormality on the D7 images, even though the predictive value of the D7 MTR analysis was less than that of the acute or the entire sample results. However, when MTR abnormality was noted on the acute scans, there was a very high likelihood of its being associated with injury proven by histopathology. This was somewhat surprising in that the D7 examination was the more proximal in time to the histopathologic examination. We speculate that our observation reflected a higher threshold of damage for injury to be detected immediately, and that early detection of injury might portend a less favorable outcome. Furthermore, it is possible that the type of injury detected by MTR on the acute studies was different from that seen on the D7 study. For example, myelin degradation has been reported to be detectable within 2 days of injury in blunt head trauma (23). In our study myelin degradation

was likely to be evolving through the entire post-injury period but may not have been extensive at the time of the acute study (approximately 3 h post injury).

Although the associations between MTR and histopathology for the entire sample as well as the acute scans were statistically significant, sometimes MTR detected pathology and histologic results did not, and vice versa. There are several possible explanations for these observations, some of which suggest ways in which the examination might be improved for future study. First, the MR slices examined were many times larger than were the histopathology sections, so it is possible that pathology showing up in the MR ''averaged'' view of the slice was not seen on the specific pathology section that represented the MR slice. The opposite result could be seen to correspond to the situation in which isolated pathology appeared on one or two sections but was not present on the bulk of the tissue that made up the slice and was thus ''averaged out.'' Similar arguments result from consideration of the vastly different ''pixel'' sizes between the two modalities, with the understanding that an area corresponding to several adjoining pixels must be affected on an MR image in order for the region to be detectable. This limitation is likely to have affected the NPV of MTR for the presence of DAI. Another possible explanation for regions in which MTR was positive while histopathology was negative is that MTR served as a non-specific indicator of structural compromise while the histopathology analyses were specific to axonal damage such as that which characterized DAI. We did not register the MR images with one another, as errors that could be corrected by registration were judged to be minor compared with the mismatch between MR slice thickness and histopathology section thickness. However, the histopathology team reported little or no difficulty in relating the images provided to the corresponding sections and was careful to perform the section slicing in the same plane as the D7 MR images.

It is known that the MTR examination requires standardization of technique and stability of the scanning equipment to be reproducible. Specifically, the average power and offset frequency of the MTR saturation pulses must be held constant to control the selectivity of the saturation (24). It is usually not problematic to control the offset frequency on clinical scanners, but precise control of the saturation power may be difficult. Scanning features such as automatic pre-scan adjustment must be prevented from inadvertently altering the power between the control and saturation scans. Coil loading and animal positioning are also potential complicating factors. Although every effort was made to standardize these parameters, the standard deviation of normal white matter values in the pre-injury studies was greater than 2% MTR, which limited the sensitivity of the technique for detection of subtle changes. The saturation parameters we employed for the MT acquisitions were previously found to provide gray-matter to white-matter contrast that was comparable to MT imaging results at 1.5 T in the identical swine model, while staying within scanner power limitations. While it was not possible to establish that the protocol was strictly optimized for detection of DAI, the method was designed to be, and evaluated as, comparable to protocols we employ for examination of human patients with suspected DAI.

This study was conducted using a whole-body scanner operating at 4 T, which is a significantly higher field strength than those commonly employed for examination of patients. The higher field was expected and verified to lengthen relaxation times and thus was expected to influence the numerical values of MTRs. In addition, as noted, variation of saturation power levels and saturation offset frequencies complicates comparison of study results with those obtained using different saturation parameters. For these reasons we adopted statistical measures to define abnormality and employed those statistical parameters in the generation of maps used to locate the abnormalities. Our results suggest that this type of comparison may contribute to increases in sensitivity of the MR examination. In addition, the methods we have presented may be useful in future studies designed to optimize acquisition techniques for specific pathologies.

We have demonstrated that MTR analysis is a useful technique for the detection of DAI in our animal model. Furthermore, our results suggest that MTR analysis may be applied, following acquisition of appropriate normative data, to individual subjects. To our knowledge, ours is the only animal model in use that is able to produce the inertial loading conditions typical of human head injury that induces DAI. Extrapolation of these results to human head injury is reasonable and straightforward. Thus, we speculate that detection of lowered MTR in the human brain following traumatic injury will be associated with the presence of diffuse axonal pathology. Future work suggested by these results includes study of more severely injured animals, to develop a range of pathology, including tissue tears, and to test for correlation between the quantitative MTR values and the pathology grades. Study of MT-abnormal regions that are pathology-normal may be extended to detect different forms of injury not visible using the immunohistochemical techniques employed. Additional studies at the injury levels at and below those employed to date may aid in definition of a tolerable level of brain acceleration that is below the threshold of pathophysiologic and pathobiologic damage. In humans, studies comparing injury detected by conventional MRI as well as MTI with clinical status and progress may be useful in the evaluation of the efficacy of new pharmacotherapies for brain injury. Finally, efforts to improve the reproducibility of the MT examination may provide benefits in the sensitivity of the technique, allowing the reliable detection of a greater fraction of the mild injury.

REFERENCES

1. Sosin D, Sacks J, Smith S. Head injury-associated deaths in the United States from 1979–1986. JAMA 1989;262:2251–2255.
2. Sosin D, Sniezek J, Waxweiler R. Trends in death associated with traumatic brain injury. JAMA 1992;273:1778–1780.
3. Gennarelli TA. Mechanisms of brain injury. J Emerg Med 1993;11(suppl 1):5–11.
4. Gennarelli TA, Thibault L, Adams H, Graham D, Thompson C, Marcincin R. Diffuse axonal injury and traumatic coma in the primate. Ann Neurol 1982;12:564–574.

5. Wolff SD, Balaban RS. Magnetization transfer contrast (MTC) and tissue water proton relaxation in vivo. Magn Reson Med 1989;10:135–144.
6. Dousset V, Grossman RI, Ramer KN, Schnall MD, Young LH, Gonzalez SF, Lavi E, Cohen JA. Experimental allergic encephalomyelitis and multiple sclerosis: lesion characterization with magnetization transfer imaging [published erratum appears in Radiology 1992;183:878]. Radiology 1992;182:483–491.
7. Lexa FJ, Grossman RI, Rosenquist AC. MR of wallerian degeneration in the feline visual system: characterization by magnetization transfer rate with histopathologic correlation. AJNR 1994;15:201–212.
8. Petrella JR, Grossman RI, McGowan JC, Campbell G, Cohen JA. Multiple sclerosis lesions: relationship between MR enhancement pattern and magnetization transfer effect. AJNR 1996;17:1041–1049.
9. Loevner LA, Grossman RI, McGowan JC, Ramer KN, Cohen JA. Characterization of multiple sclerosis plaques with T1-weighted MR and quantitative magnetization transfer. AJNR 1995;16:1473–1479.
10. Boorstein JM, Wong KT, Grossman RI, Bolinger L, McGowan JC. Metastatic lesionsof the brain: imaging with magnetization transfer. Radiology 1994;191:799–803.
11. Kasner SE, Galetta SL, McGowan JC, Grossman RI. Magnetization transfer imaging in progressive multifocal leukoencephalopathy. Neurology 1997;48:534–536.
12. Meaney JF, Watt JW, Eldridge PR, Whitehouse GH, Wells JC, Miles JB. Association between trigeminal neuralgia and multiple sclerosis: role of magnetic resonance imaging. J Neurol Neurosurg Psychiatry 1995;59: 253–259.
13. Smith D, Chen X, Xu B, McIntosh T, Gennarelli T, Meaney D. Characterization of diffuse axonal pathology and selective hippocampal damage following intertial brain trauma in the pig. J Neuropathol Exp Neurol 1997;56:822–834.
14. Meaney D, Thibault L, Smith D, Ross D, Gennarelli T. Diffuse axonal injury in the miniature pig: biomechanical development and injury threshold. ASME WAM 1993;25:169–175.
15. Greenes R, Begg C. Methodology for unbiased estimation from examples of selectively verified patients. Invest Radiol 1985;20:751–756.
16. Adams J, Graham D, Murray L, Scott G. Diffuse axonal injury due to non-missile head injury in humans: an analysis of 45 cases. Ann Neurol 1982;12:557–563.
17. Adams J. Head injury. In: Adams J, Corsellis J, Duchen L, editors. Greenfield's neuropathology, New York: John Wiley & Sons; 1984. p 85–124.
18. Adams J, Doyle D, Ford I, Gennarelli T, Graham D, McClellan D. Diffuse axonal injury in head injury: definition, diagnosis, and grading. Histopathology 1989;15:49–59.
19. Maxwell W, Watt C, Graham D. Ultrastructural evidence of axonal shearing as a result of lateral acceleration of the head in non-human primates. Acta Neuropathol 1993;86:136.
20. Povlishock J, Erb D, Astruc J. Axonal response to traumatic brain injury: reactive axonal change, deafferentation, and neuroplasticity. J Neurotrauma 1992;9:S189–S200.
21. Yaghmai A, Povlishock J. Traumatically induced reactive change as visualized through the use of monoclonal antibodies targeted to nerofilament subunits. J Neuropathol Exp Neurol 1992;51:158–176.
22. Strich S. Shearing of nerve fibers as a cause of brain damage due to head injury. A pathological study of 20 cases. Lancet 1961;2:443–448.
23. Ng H, Mahaliyana R, Poon W. The pathological spectrum of diffuse axonal injury in blunt head trauma: assessment with axon and myelin stains. Clin Neurol Neurosurg 1994;96:24–31.
24. McGowan JC, Leigh J. Selective saturation in magnetization transfer experiments. Magn Reson Med 1994;32:517–522.